NOTES AND CORRESPONDENCE

Revisiting the Thermocline Depth in the Equatorial Pacific*

HAIJUN YANG AND FUYAO WANG

Department of Atmospheric Science, School of Physics, Peking University, Beijing, China

(Manuscript received 11 September 2008, in final form 6 December 2008)

ABSTRACT

The thermocline depth is defined as the depth of the maximum vertical temperature gradient. In the equatorial Pacific, the depth of 20°C isotherm is widely used to represent the thermocline depth. This work proposes that under the circumstance of a significant mean climate shift, it is better to use the original definition of the thermocline depth in studying the long-term changes in mean climate and tropical coupled climate variabilities. For instance, during the transient period of global warming, the tropical thermocline is usually enhanced because the surface layer warms more and faster than the lower layers. The depth of maximum vertical temperature gradient shoals, which is consistent with the enhanced thermocline. However, the 20°C isotherm depth deepens, which suggests a weakened thermocline. This discrepancy exists in both the observations and the future climate simulations of coupled models.

1. Introduction

The thermocline is a layer within a body of water where the temperature changes rapidly with depth. The word ''thermocline'' first appears in the limnology literature of the late nineteenth century (Pedlosky 2006) and is then more frequently referred as a discontinuity layer or transition layer (Sverdrup et al. 1942). It was very difficult to detect the deep ocean thermocline until the bathythermograph (BT) was invented in 1940s and the expendable bathythermograph (XBT) was developed during the 1970s. Based on the definition, theoretically, the depth of thermocline (DTC) should be taken as the depth of the maximum vertical temperature gradient (Z_{tc}). However, in practice, the vertical resolution of observations is usually insufficient to resolve the maximum temperature gradient. Thus, the DTC is often determined by the depth of a ''representative'' isotherm [e.g., the depth of the 14° or 20°C isotherm (Z_{14} and Z_{20}, respectively)] within the thermocline layer (Meyers 1979a,b; Kessler 1990).

For the equatorial Pacific, Z_{20} is broadly used as the DTC for studies (Kessler 1990; Ji et al. 1995; Vialard and Delecluse 1998; Swenson and Hansen 1999; Chavez et al. 1999; Durand and Delcrolx 2000; Vecchi and Harrison 2000; Meinen and McPhaden 2000; Fedorov and Philander 2001; Chepurin et al. 2005) because the 20°C isotherm is located near the center of the main thermocline. In earlier studies, the Z_{14} was chosen to represent the permanent DTC because it indicates strength of the North and South Equatorial Currents better than shallower isotherms (Meyers 1979a), although it is below the level of the Z_{tc}. Both the Z_{20} and Z_{14} have some problems in representing the DTC (Wang et al. 2000). The Z_{20} is suitable for the warm pool, but it may fail for the cold tongue and coastal upwelling regions because the 20°C isotherm may outcrop to the surface during the cold season. On the other hand, the Z_{14} is too deep to represent the warm pool thermocline temperature. Therefore, Wang et al. (2000) proposed to use a location-dependent representative temperature T_c to characterize the thermocline temperature. The DTC is defined by averaging 12°C (representing the temperature at the base of the thermocline layer) and the local long-term mean sea surface temperature (SST; representing the temperature at the top

* Department of Atmospheric Science Contribution Number 008.

Corresponding author address: Haijun Yang, Department of Atmospheric Science, School of Physics, Peking University, 209 Chengfu Road, Beijing 100871, China.
E-mail: hjyang@pku.edu.cn

DOI: 10.1175/2009JCLI2836.1

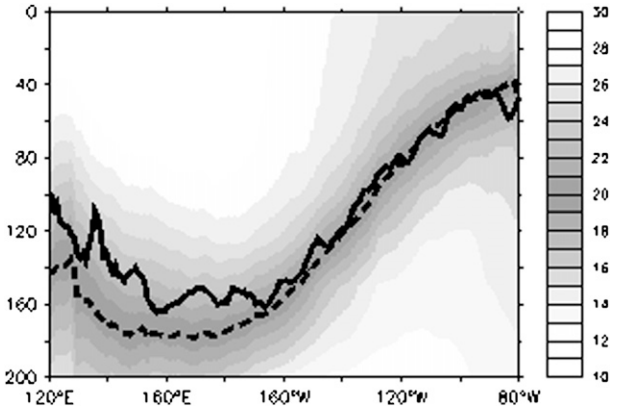

FIG. 1. Climatological annual mean upper-ocean temperature (°C) averaged between 5°S and 5°N from Levitus data (1955–2003). The dashed line shows the location of the 20°C isotherm (Z_{20}), and the solid line shows the location of the maximum vertical temperature gradient (Z_{tc}).

of the thermocline). Such defined representative temperature T_c varies from 20.5°C in the warmest places to about 16°C near the Peru coast.

The essence of wind-driven circulation is the thermocline dynamics. For the equatorial Pacific, the DTC variations play a key role in both the mean SST and the coupled climate variabilities, such as El Niño–Southern Oscillation (ENSO). The basin-wide adjustment of the equatorial thermocline, including the vertical displacement and zonal tilting, is closely related to the phase, amplitude, and time scale of the tropical variabilities (Zebiak and Cane 1987; Chang 1994; Wang et al. 2000). Because of different physical processes involved, the thermocline adjustment may exhibit distinctive features and impact differently on the SST and ENSO (Chang 1994). An optimal proxy of the DTC is therefore critical to properly understand the thermocline dynamics.

Usually, in the equatorial Pacific, the location of the maximum vertical temperature gradient Z_{tc} is best represented by Z_{20}, as suggested in most studies. The Z_{tc} and Z_{20} are well overlapped with each other except in the warm pool region where the Z_{tc} tends to be located at the upper portion of the thermocline layer (Wang et al. 2000). One of advantages of using Z_{20} is that it implies the studies of movements along an isopycnal level. The tropical Pacific may be well approximated as a two-layer system divided by the 20°C isotherm (Kessler 1990).

It is worth discussing if the Z_{20} is still the best proxy of the Z_{tc} under the circumstance of a significant mean climate shift. For instance, in the global warming, the 20°C isotherm will be intuitionally pushed downward because of the general warming in the upper layer of oceans. The Z_{tc}, instead, may move upward because the upper portion of the thermocline layer warms more and faster than the lower ocean. The opposite changes in the Z_{20} and Z_{tc} may bring discrepancy in understanding the

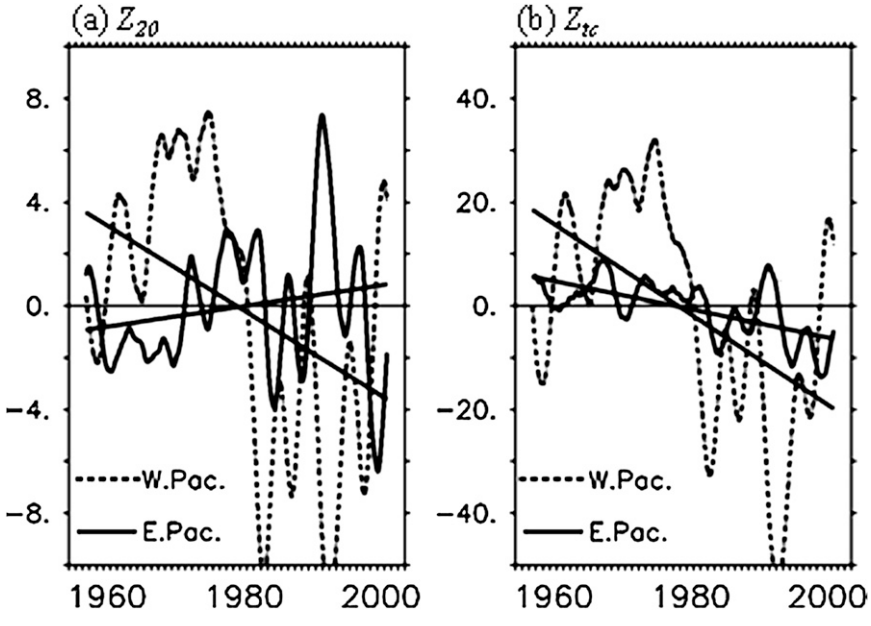

FIG. 2. Time evolution (curves) of (a) Z_{20} and (b) Z_{tc} averaged over the WEP (dashed; 5°S–5°N, 120°E–160°W) and the EEP (solid; 5°S–5°N, 130°–80°W) from the monthly JEDAC-XBT over the period 1955–2003 in meters. The climatological annual mean values of Z_{20} and Z_{tc} are removed. The linear regressions of these curves are also plotted as straight lines. The 5-yr running mean is applied to the time series lines.

TABLE 1. The values of trends and corresponding confidence intervals at the 99% significant level for the EEP Z_{20} and Z_{tc} (in m century^{-1}). The confidence interval is obtained by Student's t test. All the trends are significant at the 99% significance level. The trends are calculated from the monthly XBT data over the period of 1955–2003 and GFDL CM2.1 and NCAR CCSM3 data over years 1–70. These values are also visualized in Fig. 3.

EEP		Trend	Confidence interval
XBT (1955–2003)	Z_{20}	2.6	[0.4, 4.8]
	Z_{tc}	−27.6	[−31.2, −24.0]
GFDL (1–70)	Z_{20}	7.1	[2.6, 11.6]
	Z_{tc}	−6.8	[−8.8, −4.8]
NCAR (1–70)	Z_{20}	4.1	[2.3, 5.9]
	Z_{tc}	−2.4	[−3.8, −1.0]

impact of thermocline change on the surface coupled climate variabilities such as ENSO. If during the transient period of global warming a stronger ENSO is observed, then this could result from either an intensified or weakened equatorial thermocline (referring to Z_{tc} and Z_{20}, respectively). This discrepancy arises unnecessarily from the different treatment of the DTC. The relationship of a stronger ENSO to an intensified thermocline is widely accepted (e.g., An et al. 2008; Meehl et al. 2001; Collins 2000; Timmermann et al. 1999).

In this note, we propose that it is necessary to use the original definition of the thermocline depth to avoid this discrepancy. The vertical resolution issue is not a practical obstacle to resolve the Z_{tc} anymore, considering the great improvement in both the observations and coupled models in the past decades. Some recent works have already adopted Z_{tc} in the global warming studies (e.g., Vecchi et al. 2006). In the following context, we will show that using Z_{tc} is better for the consistencies between the thermocline dynamics and the coupled variabilities under the background of mean climate shift.

2. Data

Observational datasets examined here include 1) the monthly upper-ocean temperature dataset from the Scripps Institution of Oceanography Joint Environmental Data Analysis Center (JEDAC-XBT) and 2) the yearly ocean temperature dataset from the National Oceanographic Data Center (NODC; Levitus et al. 2005). The JEDAC-XBT data have a horizontal resolution of 5° × 2° in longitude and latitude and 11 vertical levels (0, 20, 40, 60, 80, 120, 160, 200, 240, 300, and 400; available online at http://jedac.ucsd.edu/DATA_IMAGES/index.html). The Levitus data have a horizontal resolution of 1° × 1° in longitude and latitude and 16 vertical levels (0, 10, 20, 30, 50, 75, 100, 125, 150, 200, 250, 300, 400, 500, 600, and 700). Both datasets span the period 1955–2003.

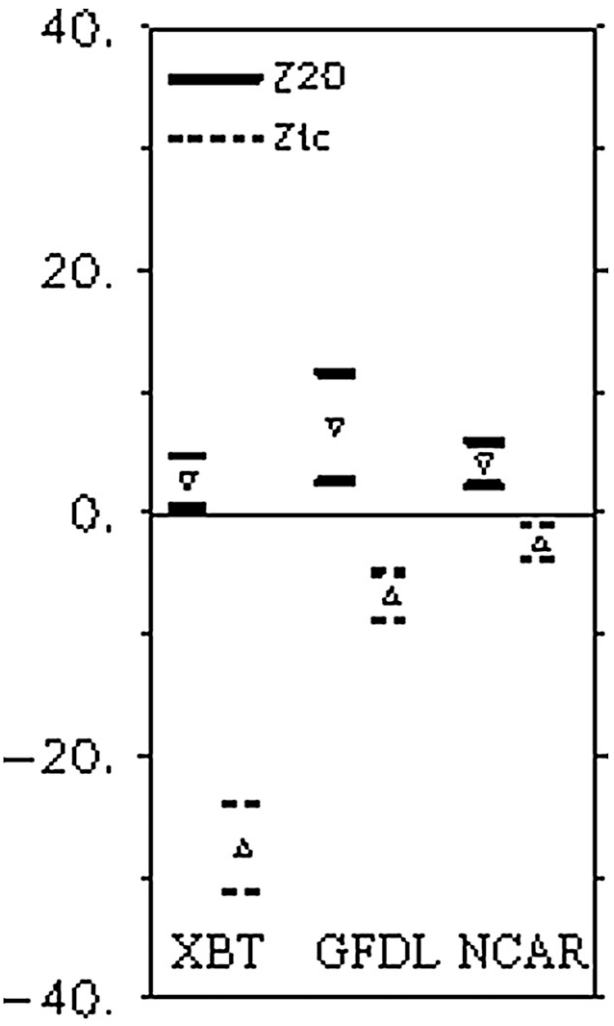

FIG. 3. The values of trends (triangles) and corresponding confidence intervals (short straight lines) at the 99% significant level for the EEP Z_{20} (dashed) and Z_{tc} (solid) in meters per century. It is seen that all the trends are significant and the trends of Z_{20} and Z_{tc} are opposite in the EEP for both the XBT data and coupled models (GFDL CM2.1 and NCAR CCSM3).

The model datasets examined here are from phase 3 of the Coupled Model Intercomparison Project (CMIP 3) evaluated for the Fourth Assessment Report (AR4) of the Intergovernmental Panel on Climate Change (IPCC): the Geophysical Fluid Dynamics Laboratory Climate Model version 2.1 (GFDL CM2.1) and the National Center for Atmospheric Research Community Climate System Model, version 3 (NCAR CCSM3). The "1% increase per year to doubling" (1pctto2x) experiments from these two models are examined. In this paper, only the first 70 yr of outputs of 1pctto2x experiments are analyzed to identify the linear change in the DTC in a future warming climate; that is, we only focus on the transient period of the global warming

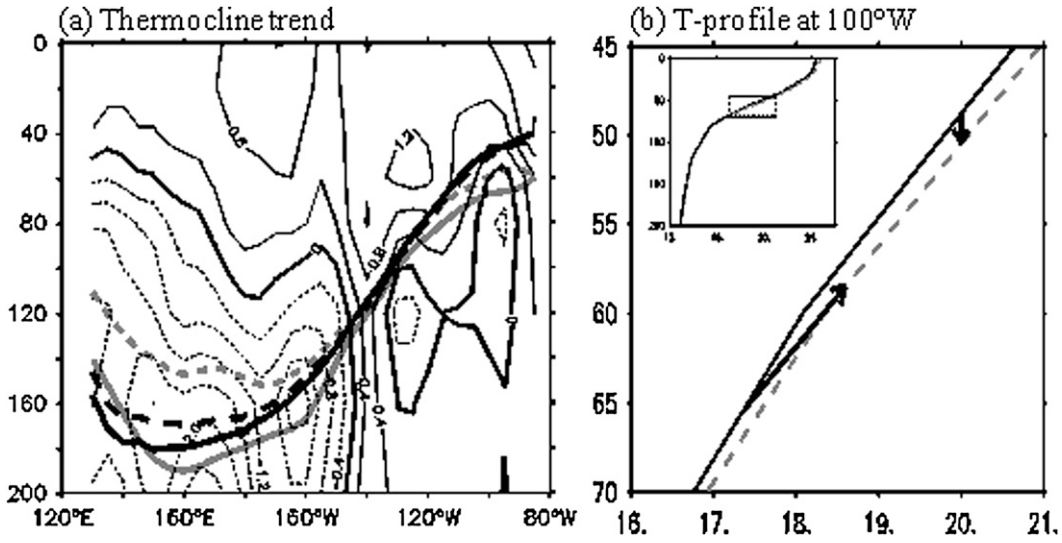

FIG. 4. (a) Linear trend of the upper-ocean temperature (°C century^{-1}) averaged between 5°S and 5°N from the monthly JEDAC-XBT over the period 1955–2003. The thick black and gray lines represent the Z_{20} and Z_{tc}, respectively. The solid (dashed) lines shows the locations of Z_{20} and Z_{tc} averaged over 1960–75 (1985–2000). (b) The vertical temperature profile at 100°W. The solid line is for 1960–75 and the dashed line is for 1985–2000. The black arrows denote the changes in direction of Z_{tc} and Z_{20}. The small inset shows the vertical temperature profile in the upper 200 m, in which the dashed box marks the region of interest.

during which the atmospheric CO_2 is increased by 1% yearly.

In this note, only the long-term linear trend of the DTC is of interest. The least squares method is used to determine the linear trends. For the time evolution of the DTC, a 5-yr running mean is applied to both the observational and model data before the linear trend calculation. Furthermore, a Student's t test is used to test the significance of the linear trends (see appendix for details).

3. Mean thermocline depth in the equatorial Pacific

The Z_{tc} and Z_{20} in the equatorial Pacific generally coincide with each other, except in the warm pool region where the Z_{tc} is shallower than the Z_{20} by about 20–40 m (Fig. 1). Here, the climatological annual mean Levitus data are analyzed because of their relatively higher vertical resolution than XBT data. In the eastern Pacific, where the thermocline dynamics is vital to the SST and coupled variabilities, the Z_{20} can fully represent the Z_{tc}. In the western Pacific, where the thermocline is deep, the discrepancy between the Z_{20} and Z_{tc} does not matter because the thermocline hardly affects the surface locally. Therefore, representing the Z_{tc} with Z_{20} will not bring dynamical inconsistency for a climate with a steady time mean state, as shown in many previous studies.

4. Different changes in Z_{20} and Z_{tc}

The Z_{tc} and Z_{20} in the equatorial Pacific can change in different directions if the mean climate has a significant shift. Figure 2 shows the linear trends of the equatorial thermocline depth during 1955–2003. For the western equatorial Pacific (WEP; 5°S–5°N, 120°E–160°W), the Z_{20} and Z_{tc} exhibit the similar shoaling trend during the past half century (black lines in Figs. 2a,b). However, for the eastern equatorial Pacific (EEP; 5°S–5°N, 130°–80°W), the Z_{20} shows a deepening trend whereas the Z_{tc} shows a shoaling trend (black lines in Figs. 2a,b). Considering negative correlation between the thermocline strength and its depth in the EEP, the deepening of Z_{20} means a weakening thermocline, whereas the shoaling of Z_{tc} means a strengthening thermocline. An obvious inconsistency in understanding the thermocline dynamics occurs here. Figure 2 is plotted using monthly JEDAC-XBT. The same situation also occurs in the yearly Levitus data (figure not shown).

These trends in the equatorial DTC are significant at the 99% level (Table 1; Fig. 3). The Student's t test is used to test the significance. The trends in the WEP are remarkable, as shown in Fig. 2. For simplicity and clarity only, the values in the EEP are listed in Table 1 and plotted in Fig. 3. It is seen clearly that the lower and upper limits of the confidence intervals have the same sign, suggesting the significance of the linear trends. Moreover, the trends of Z_{20} and Z_{tc} are clearly opposite of each other.

There is evidence showing that the global ocean has been warming for a long time (Levitus et al. 2005; Vecchi et al. 2006). The warming rate of tropical SST in

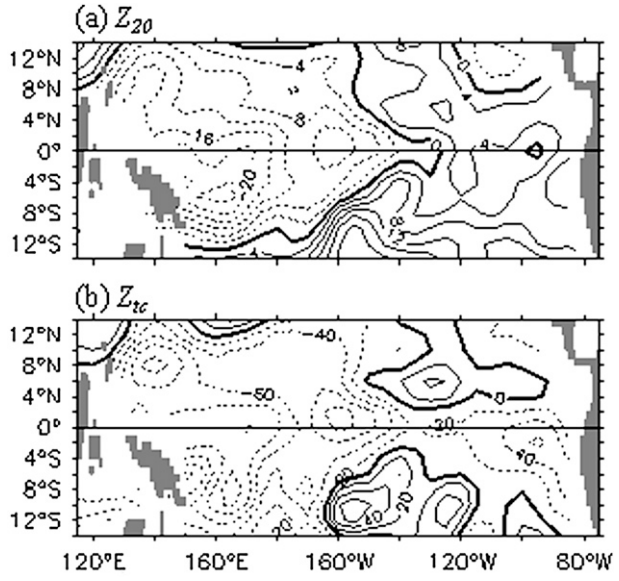

FIG. 5. Linear trends of (a) Z_{20} and (b) Z_{tc} (m century^{-1}) in the tropical Pacific from the monthly JEDAC-XBT over the period 1955–2003.

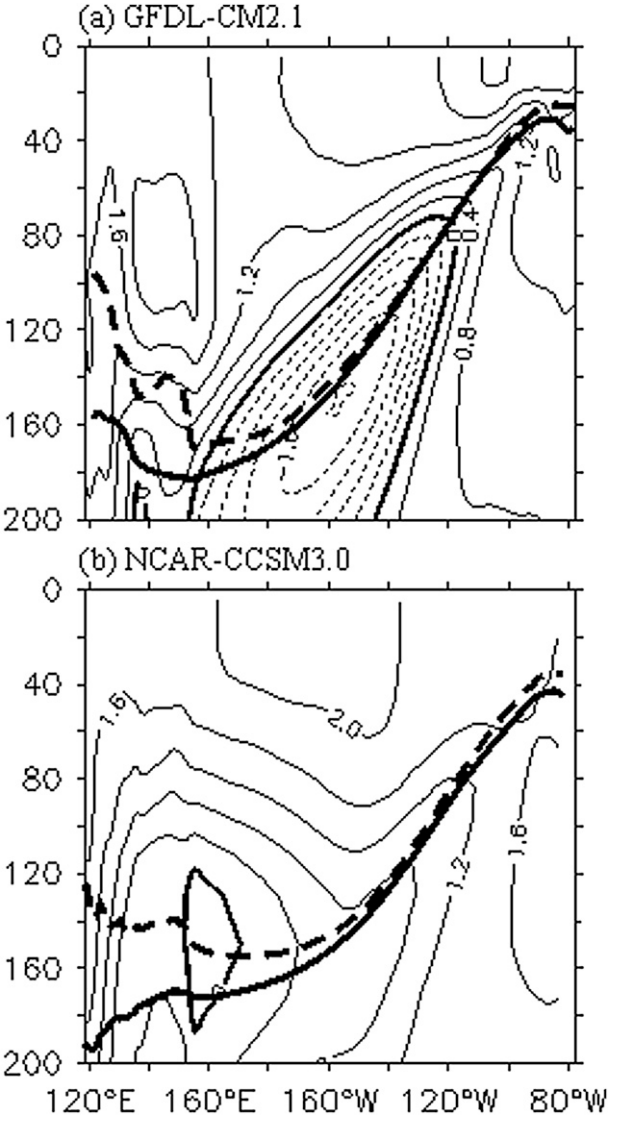

FIG. 6. Linear trends of the upper-ocean temperature (°C century^{-1}) averaged between 5°S and 5°N from the 1pctto2x experiments of (a) GFDL CM2.1 and (b) NCAR CCSM3 over years 1–70. The thick solid and dashed lines in (a) and (b) represent the time averaged Z_{20} and Z_{tc} over years 1–70, respectively.

the past 50 yr is generally over 1°C century^{-1}; it reaches 1.5°C century^{-1} in the EEP (Fig. 4a). This big surface warming, however, has not penetrated sufficiently deep into the thermocline, where a cooling trend occurs instead. The cooling rate in the western thermocline reaches as much as −2°C century^{-1}. Although the cooling rate in the eastern thermocline is not as significant as that in the west, the overall vertical temperature gradient is enhanced during the past 50 yr. This clearly shows a strengthening trend in the equatorial Pacific thermocline.

The different trends in the Z_{20} and Z_{tc} can be also seen in Fig. 4. Because of the overall surface warming, the 20°C isotherm level has to be pushed downward. Because of the much faster warming in the surface layer than in the subsurface, the location of the maximum vertical temperature gradient has to move upward so that the Z_{tc} has a shoaling trend in the eastern Pacific (Fig. 4b). The real situation that happened in the EEP is that the thermocline is strengthening and shoaling as disclosed by Z_{tc} instead of weakening and deepening as suggested by Z_{20}.

Figure 4a also shows an overall reduction in the Z_{tc} and Z_{20} in the equatorial Pacific. The shoaling trend of the DTC is more notable in the western equatorial Pacific than in the east, suggesting a flattening in the east–west tilt of the equatorial Pacific thermocline (Fig. 4a). The horizontal pattern of Z_{20} trend clearly shows a zonally flattening thermocline with a shoaling in the west and a deepening in the east (Fig. 5a), whereas the horizontal pattern of Z_{tc} shows a zonal shoaling and flattening in the whole equatorial Pacific (Fig. 5b). The flattening of the equatorial thermocline can be attributed to the weakened trade wind and, therefore, the weakening of tropical Walker circulation (Vecchi et al. 2006; Vecchi and Soden 2007). It is worth noting that the magnitude of the Z_{tc} trend is much larger than that of the Z_{20} trend: about 5 times more in the west and about 10 times more in the east. This implies that the significant change in the thermocline depth could be incorrectly ignored if the focus is only on the Z_{20}.

The shoaling of Z_{tc} (i.e., the strengthened thermocline in the EEP) is consistent with the enhancing

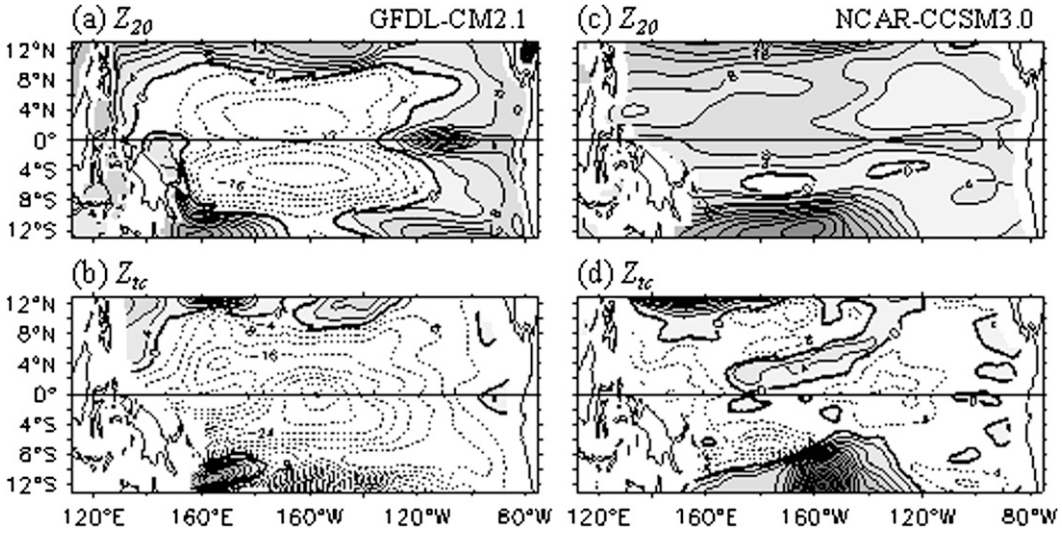

FIG. 7. Linear trends of (a),(c) Z_{20} and (b),(d) Z_{tc} (m century^{-1}) in the tropical Pacific from the 1pctto2x experiments of (left) GFDL CM2.1 and (right) NCAR CCSM3 over years 1–70.

ENSO amplitude in the past 50 yr (Yang and Zhang 2008). The shoaling of Z_{tc} increases the SST sensitivity to the thermocline in the Niño-3 region (5°S–5°N, 150°–90°W; Philip and van Oldenborgh 2006). A shallower Z_{tc} means the thermocline water would be easier to affect the SST through the anomalous upwelling. A stronger thermocline means a bigger impact on the SST. The shallower and stronger thermocline can result in an enhanced ENSO variability because of the positive feedback among the wind variability, anomalous upwelling, and SST variability in the central-east Pacific (Yang and Zhang 2008). If the Z_{20} is used to represent the DTC in this situation, a false dynamic connection between the DTC and ENSO changes would be concluded.

Here, we further check the DTC change in 1pctto2x experiments of two coupled models: GFDL CM2.1 and NCAR CCSM3. Because coupled models are the most important tools in climate studies, the proper treatment of the equatorial thermocline in coupled models is crucial to correctly understand the mechanisms of the tropical climate variabilities. Figure 6 shows that, during the transient stage of global warming, the equatorial thermocline is enhanced in both of the models and the mean Z_{tc} is usually shallower than the mean Z_{20}. It is seen that, in the EEP, the Z_{20} has a deepening trend (Figs. 7a,c), whereas the Z_{tc} has a shoaling trend (Figs. 7b,d). The Z_{tc} differs from the Z_{20} in both the sign and size. The deepening of Z_{20} should suggest a weakening thermocline, particularly in the eastern Pacific; however, the trend in the upper-ocean temperature (Fig. 6) suggests that the thermocline is enhanced during the transient stage of global warming, which is consistent with the shoaling of Z_{tc}, as shown in Figs. 7b,d. Moreover, conformed to the enhancing thermocline, ENSO amplitude is also increased in these two coupled models (figure not shown). This has been examined carefully in Yang and Zhang (2008). The change in ENSO amplitude is well complied with the change in Z_{tc} in dynamics. Therefore, the Z_{tc} is better to reflect the real changes in the equatorial thermocline and should be paid more attention in the study of the tropical coupled climate variabilities, particularly under the circumstance of mean climate shift.

The significance of these trends in the two models is also checked. All the trends are significant at the 99% confidence level (Table 1). It is noticed that the shoaling trend of the Z_{tc} in the EEP is much smaller than that in the observation (Fig. 3). This is consistent with the relatively weaker changes in the equatorial thermocline strength suggested in Fig. 6 than those in the XBT (Fig. 4a). In the coupled models, the warming trends in the EEP penetrate much deeper than those in the XBT, whereas the cooling trends mostly occur to the west of 130°W (Figs. 6a,b). This is responsible for the smaller Z_{tc} changes in the coupled model (Fig. 3). As for what causes the vertical temperature structures in the coupled models as shown in Fig. 6, we have to turn to a thorough examination of the coupled models simulations, which is outside of the discussions of this work.

5. Summary

The analyses above remind us that we should be cautious when investigating the long-term change in the

equatorial thermocline and its impact on the surface dynamics. The different treatment of the DTC may result in controversies in understanding the mechanisms of the coupled climate variabilities in the tropics. Although using Z_{20} to represent the DTC has many advantages (e.g., it is the most convenient and simplest method to determine the DTC in the tropical Pacific and it simplifies the three-dimensional variability into a two-dimensional field, which can be mapped and studied conveniently; Kessler 1990), Z_{20} may fail to reflect the realistic long-term trend of the thermocline strength. Identifying the change in the depth of the maximum vertical temperature gradient is of great necessity in understanding the long-term climate change properly.

To avoid some unnecessary discrepancies, it is particularly important to figure out if Z_{20} or Z_{tc} is better to represent the DTC in the tropical Pacific when studying the past or future climate change by coupled models, because the changes in Z_{20} and Z_{tc} can be out of phase along the equator in the situation of global warming or cooling. Some of recent modeling studies have already used Z_{tc} (e.g., Vecchi et al. 2006). Considering the great improvement of the vertical resolution of coupled models, reasonably identifying Z_{tc} no longer has any practical obstacles.

Acknowledgments. This work is jointly supported by the NSF of China (No. 40576004) and the National Basic Research Program of China (2007CB411801). The comments from two anonymous reviewers are greatly appreciated. We thank the international groups for providing observational data and coupled model outputs.

APPENDIX

Linear Trend and Student's *t* Test

A linear regression line for a random sample $y(x)$ can be represented as $y = bx + a$. Here, x is the independent variable and y is the dependent variable. For convenience, we introduce S_{xx} and S_{yy} as the variances of variables x and y, respectively, and S_{xy} as the covariance of x and y as follows:

$$S_{xx} = \sum_{i=1}^{n} (x_i - \overline{x})^2, \quad S_{yy} = \sum_{i=1}^{n} (y_i - \overline{y})^2, \quad \text{and}$$
$$S_{xy} = \sum_{i=1}^{n} (x_i - \overline{x})(y_i - \overline{y}). \tag{A1}$$

The slope (i.e., the linear trend) can then be calculated by the formula $\hat{b} = S_{xy}/S_{xx}$, according to the least squares method.

The significance of the linear trend can be tested as follows: First, the sum of square errors is calculated as $Q_e = S_{yy} - \hat{b}S_{xy}$. If the variance of the error term is denoted by σ^2, then an unbiased estimate of σ^2 can be given by $\hat{\sigma}^2 = Q_e/(n-2)$.

Second, the test statistic is defined as the following:

$$T = \frac{\hat{b} - b_0}{\hat{\sigma}/\sqrt{S_{xx}}}, \tag{A2}$$

where b_0 is given. For the two-tailed t test H_0:$b_0 = 0$ and H_1:$b_0 \neq 0$. Under the significant level α, the rejection region for H_0 is the following:

$$\frac{|\hat{b}|}{\hat{\sigma}} \sqrt{S_{xx}} \geq t_{\alpha/2}(n-2). \tag{A3}$$

Therefore, the $(1-\alpha)$ percent confidence interval for the slope (linear trend) is the following:

$$\hat{b} \pm t_{\alpha/2}(n-2) \times \frac{\hat{\sigma}}{\sqrt{S_{xx}}}. \tag{A4}$$

REFERENCES

An, S.-I., J.-S. Kug, Y.-G. Ham, and I.-S. Kang, 2008: Successive modulation of ENSO to the future greenhouse warming. *J. Climate,* **21,** 3–21.

Chang, P., 1994: A study of the seasonal cycle of sea surface temperature in the tropical Pacific Ocean using reduced gravity models. *J. Geophys. Res.,* **99,** 7725–7741.

Chavez, F. P., P. G. Strutton, G. E. Friederich, R. A. Feely, G. C. Feldman, D. G. Foley, and M. J. McPhaden, 1999: Biological and chemical response of the equatorial Pacific ocean to the 1997-98 El Niño. *Science,* **286,** 2126–2131.

Chepurin, G. A., J. A. Carton, and D. Dee, 2005: Forecast model bias correction in ocean data assimilation. *Mon. Wea. Rev.,* **133,** 1328–1342.

Collins, M., 2000: The El Niño–Southern Oscillation in the second Hadley Centre coupled model and its response to greenhouse warming. *J. Climate,* **13,** 1299–1312.

Durand, F., and T. Delcroix, 2000: On the variability of the tropical Pacific thermal structure during the 1979–96 period, as deduced from XBT sections. *J. Phys. Oceanogr.,* **30,** 3261–3269.

Fedorov, A. V., and S. G. Philander, 2001: A stability analysis of tropical ocean–atmosphere interaction: Bridging measurements and theory for El Niño. *J. Climate,* **14,** 3086–3101.

Ji, M., A. Leetmaa, and J. Derber, 1995: An ocean analysis system for seasonal to interannual climate studies. *Mon. Wea. Rev.,* **123,** 460–481.

Kessler, W. S., 1990: Observations of long Rossby waves in the northern tropical Pacific. *J. Geophys. Res.,* **95,** 5183–5217.

Levitus, S., J. Antonov, and T. Boyer, 2005: Warming of the world ocean, 1955–2003. *Geophys. Res. Lett.,* **32,** L02604, doi:10.1029/2004GL021592.

Meehl, G. A., P. R. Gent, J. M. Arblaster, B. L. Otto-Bliesner, E. C. Brady, and A. Craig, 2001: Factors that affect the amplitude of El Niño in global coupled climate models. *Climate Dyn.,* **17,** 515–526.

Meinen, C. S., and M. J. McPhaden, 2000: Observations of warm water volume changes in the equatorial Pacific and their relationship to El Niño and La Niña. *J. Climate,* **13,** 3551–3559.

Meyers, G., 1979a: On the annual Rossby wave in the tropical North Pacific Ocean. *J. Phys. Oceanogr.,* **9,** 663–674.

——, 1979b: Annual variation in the slope of the 14° isotherm along the equator in the Pacific Ocean. *J. Phys. Oceanogr.,* **9,** 885–891.

Pedlosky, J., 2006: A history of thermocline theory. *Physical Oceanography: Developments since 1950,* M. Jochum and R. Murtugudde, Eds., Springer, 139–152.

Philip, S., and G. J. van Oldenborgh, 2006: Shifts in ENSO coupling processes under global warming. *Geophys. Res. Lett.,* **33,** L11704, doi:10.1029/2006GL026196.

Sverdrup, H. U., M. W. Johnson, and R. H. Fleming, 1942: *The Oceans: Their Physics, Chemistry, and General Biology*. Prentice-Hall, 1087 pp.

Swenson, M. S., and D. V. Hansen, 1999: Tropical Pacific Ocean mixed layer heat budget: The Pacific cold tongue. *J. Phys. Oceanogr.,* **29,** 69–81.

Timmermann, A., M. Latif, A. Bacher, J. Oberhuber, and E. Roeckner, 1999: Increased El Niño frequency in a climate model forced by future greenhouse warming. *Nature,* **398,** 694–696.

Vecchi, G. A., and D. E. Harrison, 2000: Tropical Pacific sea surface temperature anomalies, El Niño, and equatorial westerly wind events. *J. Climate,* **13,** 1814–1830.

——, and B. J. Soden, 2007: Global warming and the weakening of the tropical circulation. *J. Climate,* **20,** 4316–4340.

——, ——, A. T. Wittenberg, I. M. Held, A. Leetmaa, and M. J. Harrison, 2006: Weakening of tropical Pacific atmospheric circulation due to anthropogenic forcing. *Nature,* **441,** 73–76.

Vialard, J., and P. Delecluse, 1998: An OGCM study for the TOGA decade. Part II: Barrier-layer formation and variability. *J. Phys. Oceanogr.,* **28,** 1089–1106.

Wang, B., R. Wu, and R. Lukas, 2000: Annual adjustment of the thermocline in the tropical Pacific Ocean. *J. Climate,* **13,** 596–616.

Yang, H., and Q. Zhang, 2008: Anatomizing the ocean role in ENSO changes under global warming. *J. Climate,* **21,** 6539–6555.

Zebiak, S. E., and M. A. Cane, 1987: A model El Niño–Southern Oscillation. *Mon. Wea. Rev.,* **115,** 2262–2278.